Original research paper
UDC 621.372.8:[519.852:621.316
DOI 10.7251/IJEEC2002051B

Experimental, analytical and numerical analysis of voltage distribution along the cap-and-pin insulators

Mladen Banjanin

Faculty of Electrical Engineering East Sarajevo, University of East Sarajevo, East Sarajevo, Bosnia and Herzegovina

E-mail address: mladen.banjanin@etf.ues.rs.ba

Abstract—**This paper deals with the experimental, analytical and numerical analysis of voltage distribution along the cap-and-pin insulators. Five different insulators strings are analyzed, consisting of two, three, four, five and six cap-and-pin U40BL glass disc insulators. Experimental measurements are performed in the high voltage laboratory at the Faculty of Electrical Engineering East Sarajevo. Measurement of the voltage distribution along the disc insulators is performed by using measuring sphere gap. Analytical calculations are performed by using mathematical model which considers parasite self-capacitances of disc insulators, as well as their parasite capacitances to the earth and to the phase conductor. Calculations of the parasite capacitances values are performed and optimum values which lead to the minimum difference between measured and calculated results are suggested. Numerical analyses of the non-linear voltage distribution are performed by using electrostatic field model in software Comsol Multyphisics. 2D axisymmetric models of the cap-and-pin insulators are developed. Despite the measuring configuration is not suitable for numerical analysis, relatively good agreement between the measured results and results calculated by using specialized software are achieved.**

Keywords-voltage distribution; cap-and-pin insulator; experimental measurement; analytical calculation, numerical calculation

I. INTRODUCTION

Non-linear voltage distribution along the cap-and-pin insulators exist both under the AC and DC voltages [1],[2]. This effect is caused by the parasite capacitances from the disc insulators to the earth, tower, cross-arm and to the phase conductor. Because of that, discs of the cap-and-pin insulator near the phase conductor are exposed to the larger electric field and consequently has larger voltage drop than disc insulators which are at the middle of the string, or near the grounded electrode [1],[3]. This effect reduces insulator flashover voltage, especially in the case of contaminated environment, as industrial areas, coastal areas etc. [4],[5]. In the case when disc insulator surface is contaminated, it is exposed to the larger leakage current, especially if layer of contamination is wet. Leakage current causes drying of the contamination layer. At the drained areas large electric field exists and it can cause formation of the short sparks. If the electric spark resistance is lower than the resistance of contaminated layer, sparks will lengthen until flashover at the insulator appear [6]. Because of that, it is important to obtain almost linear voltage distribution along the insulator strings, especially of those with rated voltages of ≥220 kV. That is done by using voltage grading electrodes of different shapes, for example ring electrodes [3],[7]. Voltage grading electrodes are typically placed near the phase conductor (high voltage electrode), but in some cases additional electrode is placed at the grounded side of the insulator. Non-linear voltage distribution also exists along the polymer insulators, but it is less pronounced than in the case of cap-and-pin insulators [8]. Also, because of the hydrophobic surface of the polymer insulators it is much more difficult for partial arcs to appear and to lengthen and cause flashover in comparison with glass or ceramic insulators strings [9].

In this paper the experimental, analytical and numerical analysis of the voltage distribution along the five different cap-and-pin insulators are presented. Analyzed insulator strings consist of two, three, four, five and six cap-and-pin U40BL glass disc insulators. Experimental measurement is performed by using simple and low-cost measuring equipment. Analytical mathematical model is presented in detail and can be easily understood and applied. Numerical analysis is performed in the Comsol Multyphisics [10] software by using electrostatic 2D axisymmetric models. The most important aspect of this paper is that it summarizes all three types of analysis (experimental, analytical, numerical), while most of the papers from literature perform only some of them, for example analytical analysis [11], numerical analysis [7], experimental and numerical analysis [1], or experimental and analytical analysis [12]. Additional important aspect is that equivalent circuit and measuring procedure are deeply explained and can be easily understood and reused by other authors, what is mainly not the case in similar papers [12].

II. MEASUREMENT OF THE VOLTAGE DISTRIBUTION ALONG THE CAP-AND-PIN INSULATORS

Electric circuit used for the generation of the high test voltage is given in Fig. 1 [13]. Maximum output voltage of the test transformer is 125 kV, while its maximum apparent power is 20 kVA.

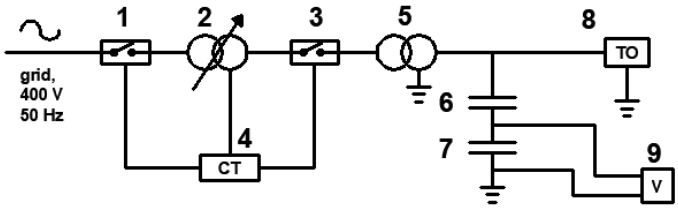

Figure 1. Electric circuit used for the generation of the high test voltage

Marks in Fig. 1 have following meanings: 1 – main switch, 2 – regulating transformer, 3 – operating switch, 4 – control table, 5 – test transformer, 6 and 7 – capacitive voltage divider, high voltage and low voltage unit respectively, 8 – test object, cap-and-pin insulator, 9 - voltmeter.

Voltage distribution along the cap-and-pin insulators is commonly measured by using measuring sphere gap [1],[13]. First step when conducting measurement is to estimate flashover voltage of the measuring sphere gap. Diameter of the applied measuring spheres is equal to 2.5 cm, while their interelectrode distance is equal to 3 mm. According to the available technical documentation, parasite capacitance of used measuring sphere gap is about 2 pF. Considering that parasite capacitance of the disc insulator is about 40 pF, as estimated in section III, measuring sphere gap connected in parallel to the disc insulator will increase its capacitance to about 42 pF, or by 5%. That is acceptable and do not lead to the significant error in measurement.

Tested insulators strings are composed of U40BL glass disc insulators. Photo of the U40BL glass disc insulator is given in Fig. 2 a), while schematic representation of the same insulator is given in Fig. 2 b).

a)

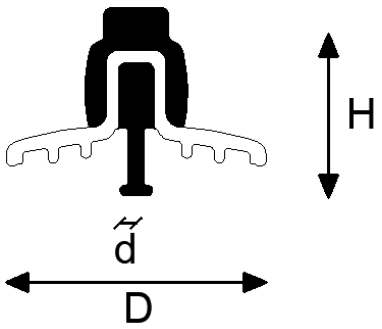

b)

Figure 2. a) Photo and b) schematic representation of the U40BL glass disc insulator

In Fig. 2 b), black color marks cap-and-pin of the insulator made of aluminum whose relative permittivity is equal to 1, while other part of the disc insulator is made of glass whose relative permittivity is equal to 4.2. In cap-and-pin disc insulators thin layer of the cement is used to improve connection between aluminum and glass [7], but in this paper it is neglected because of the unknown exact cross-section dimensions of the disc insulator.

Main dimensions and data about U40BL cap-and-pin disc insulator are given in Table I [13]. Marks in Table I are correlated with Fig. 2 b).

TABLE I. MAIN DIMENSIONS AND DATA ABOUT U40BL GLASS DISC INSULATOR

Main dimensions, Fig. 2 b)	H=110 mm, D=175 mm, d=11 mm	
1 min, 50 Hz withstand voltage	55 kV (dry)	30 kV (wet)
1.2/50 μs impulse withstand voltage	75 kV	

Flashover voltage of the measuring sphere gap can be measured as illustrated in Fig. 3. Photo of the measuring sphere gap placed at the cap-and-pin insulator composed of three disc insulators is given in Fig. 3 a) [13]. Schematic representation of the measuring configuration is given in Fig. 3 b). One electrode of the measuring sphere gap is connected to the test high voltage, while second electrode is grounded.

a)

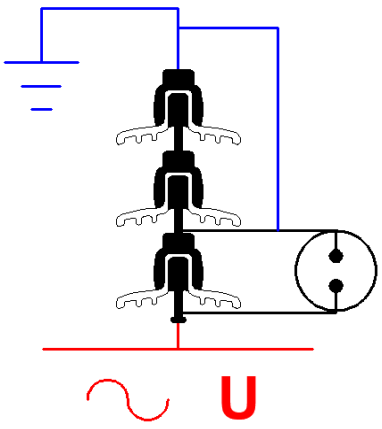

b)

Figure 3. a) Photo and b) schematic representation of the measuring configuration used for estimation of the sphere gap flashover voltage

Measured values of the sphere gap flashover voltage and calculated mean value of the flashover voltage are given in Table II. Mean value of the flashover voltage (U_{mean}=10.2 kV) is calculated by using equation (1):

$$U_{50\%} = \frac{\sum_{i=1}^{n} U_i}{n} \quad (1)$$

where: U_i is flashover voltage RMS value [kV], n – number of useful tests, 5 in this case.

TABLE II. MEASURED VALUES OF THE SPHERE GAP FLASHOVER VOLTAGE

Test number	1	2	3	4	5	**U_{mean}**
Flashover voltage [kV]	10.5	10.5	10	10	10	**10.2 kV**

In the next step, test high voltage is connected to the entire cap-and-pin insulator, as presented in Fig. 4. Photo of the experimental setup for the case of insulator string consisting of three disc insulators is given in Fig. 4 a) [13], while schematic representation of the measuring configuration is given in Fig. 4 b).

a)

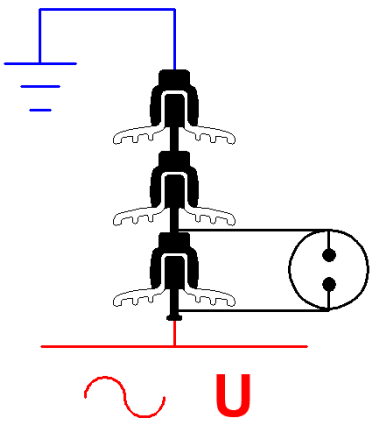

b)

Figure 4. a) Photo and b) schematic representation of the measuring configuration used for estimation of voltage distribution along the cap-and-pin insulator

Test high voltage was increased until the flashover at the measuring sphere gap appear. Five measurement was conducted for each disc insulator, and mean value was calculated by using equation (1). Position of the measuring sphere gaps was varied from top to the bottom disc insulator. Relative voltage drop at the i-th disc insulator, marked with u_i, was calculated by using equation (2):

$$u_i = \frac{U_{mean}}{U_i} \cdot 100\% \quad (2)$$

where: U_{mean} is the mean value of the measuring sphere gap flashover voltage, value of 10.2 kV is calculated in Table II, U_i is maximum RMS value of high test voltage before flashover between the measuring sphere gaps.

Measured values of the voltage distribution along the cap-and-pin insulators are given in Table III. Errors in Table III represents difference between 100%, which is equivalent to the applied test voltage, and sum of the voltage drops in % at the disc insulators. Estimated errors are acceptable and measurement results can be characterized as correct. However, sum of the partial voltage drops at disc insulators is not equal to 100%, because of the errors caused by voltage reading at the analog voltmeter, by impact of the measuring sphere gap parasite capacitance on the voltage distribution along the insulator, by deviation of the measuring sphere gap flashover voltage etc.

TABLE III. MEASURED VOLTAGE DISTRIBUTION ALONG THE CAP-AND-PIN INSULATORS

Disc number	**Voltage distribution at cap-and-pin insulator [%]**				
	Number of disc insulators in the insulator string				
	II discs	III discs	IV discs	V discs	VI discs
I*	46.79	32.90	22.67	17.35	14.43
II	52.04	29.57	21.03	15.57	12.59
III		35.17	23.34	16.45	12.86
IV			31.88	21.16	15.16
V				27.79	17.29
VI					26.36
Σ	98.83	97.64	98.91	98.33	98.68
Error	1.17	2.36	1.09	1.67	1.32

I* - disc insulator near the earthed electrode

III. ANALYTICAL CALCULATION OF THE VOLTAGE DISTRIBUTION ALONG THE CAP-AND-PIN INSULATORS

Analytical calculations of the voltage distribution along the cap-and-pin insulators are performed by using equivalent circuit with parasite capacitances [11],[13]. Such equivalent circuit for typical cap-and-pin insulator, as that in Fig. 5 a), is presented in Fig. 5 b) [13]. In this paper it is assumed that capacitances C, C_Z and C_P are equal for all disc insulators (along the insulator) in order to simplify estimation of their values [13],[14]. In some papers different values of these capacitances are calculated for different disc insulators in string [12], in order to improve accuracy of the calculated results. In addition to this model implemented with parasite capacitances, some papers suggest mathematical model based on the distributed parameters [11],[14].

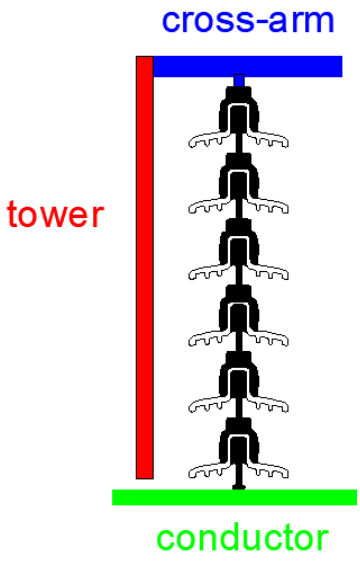

a)

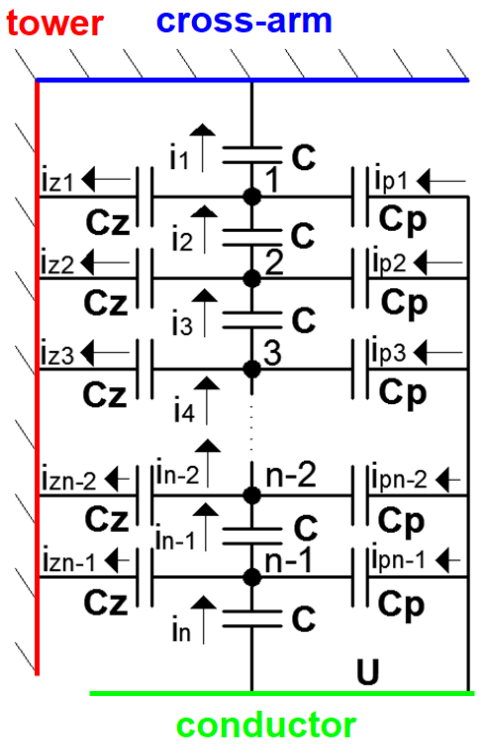

b)

Figure 5. a) Cap-and-pin insulator and b) its equivalent analytical model based on parasite capacitances

Marks in Figure 5 b) have following meanings: C_Z – parasite capacitances to the tower, cross-arm and earth, i_Z – capacitive current through C_Z, C_P – parasite capacitances to the phase conductor, i_P – capacitive current through C_P, C – parasite capacitances of the disc insulators, i – capacitive current through C, n – number of disk insulators in the insulator string, U – RMS value of the test voltage.

In the case of power frequency voltage, following complex equations can be written [13]:

$$\begin{aligned}
\underline{I}_1 + \underline{I}_{Z1} &= \underline{I}_2 + \underline{I}_{P1} \\
\underline{I}_2 + \underline{I}_{Z2} &= \underline{I}_3 + \underline{I}_{P2} \\
\underline{I}_3 + \underline{I}_{Z4} &= \underline{I}_4 + \underline{I}_{P3} \\
&\vdots \\
\underline{I}_{n-2} + \underline{I}_{Zn-2} &= \underline{I}_{n-1} + \underline{I}_{Pn-2} \\
\underline{I}_{n-1} + \underline{I}_{Zn-1} &= \underline{I}_n + \underline{I}_{Pn-1}
\end{aligned} \tag{3}$$

$$\begin{aligned}
\underline{I}_1 &= j\omega C \underline{U}_1 \\
\underline{I}_2 &= j\omega C \left(\underline{U}_2 - \underline{U}_1\right) \\
\underline{I}_3 &= j\omega C \left(\underline{U}_3 - \underline{U}_2\right) \\
&\vdots \\
\underline{I}_{n-1} &= j\omega C \left(\underline{U}_{n-1} - \underline{U}_{n-2}\right) \\
\underline{I}_n &= j\omega C \left(\underline{U} - \underline{U}_{n-1}\right)
\end{aligned} \tag{4}$$

$$\begin{aligned}
\underline{I}_{Z1} &= j\omega C_Z \underline{U}_1 \\
\underline{I}_{Z2} &= j\omega C_Z \underline{U}_2 \\
\underline{I}_{Z3} &= j\omega C_Z \underline{U}_3 \\
&\vdots \\
\underline{I}_{Zn-2} &= j\omega C_Z \underline{U}_{n-2} \\
\underline{I}_{Zn-1} &= j\omega C_Z \underline{U}_{n-1}
\end{aligned} \tag{5}$$

$$\begin{aligned}
\underline{I}_{P1} &= j\omega C_P \left(\underline{U} - \underline{U}_1\right) \\
\underline{I}_{P2} &= j\omega C_P \left(\underline{U} - \underline{U}_2\right) \\
\underline{I}_{P3} &= j\omega C_P \left(\underline{U} - \underline{U}_3\right) \\
&\vdots \\
\underline{I}_{Pn-2} &= j\omega C_P \left(\underline{U} - \underline{U}_{n-2}\right) \\
\underline{I}_{Pn-1} &= j\omega C_P \left(\underline{U} - \underline{U}_{n-1}\right)
\end{aligned} \tag{6}$$

where: $\underline{I}_1, \underline{I}_2, ..., \underline{I}_n$ are currents through parasite capacitances C of the disc insulators, $\underline{I}_{Z1}, \underline{I}_{Z2}, ..., \underline{I}_{Zn-1}$ are currents through parasite capacitances to the earth C_Z, $\underline{I}_{P1}, \underline{I}_{P2}, ..., \underline{I}_{Pn-1}$ are currents through parasite capacitances to the phase conductor C_P, $\underline{U}_1, \underline{U}_2, ..., \underline{U}_{n-1}, \underline{U}$ are voltages of nodes 1, 2, …, n-1 to the tower.

By combining equations (3), (4), (5), (6) and considering that all voltages $\underline{U}_1, \underline{U}_2, ..., \underline{U}_{n-1}, \underline{U}$ are in phase, matrix equation (7) can be written [13]:

$$[U] = [C]^{-1} \cdot [C_1] \cdot U \tag{7}$$

where:

$$[C]=\begin{bmatrix} C_E & -C & 0 & 0 & 0 & \cdots & 0 & 0 & 0 & 0 \\ -C & C_E & -C & 0 & 0 & \cdots & 0 & 0 & 0 & 0 \\ 0 & -C & C_E & -C & 0 & \cdots & 0 & 0 & 0 & 0 \\ \vdots & \vdots & \vdots & \vdots & \vdots & \cdots & \vdots & \vdots & \vdots & \vdots \\ 0 & 0 & 0 & 0 & 0 & \cdots & 0 & -C & C_E & -C \\ 0 & 0 & 0 & 0 & 0 & \cdots & 0 & 0 & -C & C_E \end{bmatrix}$$

$$C_E = 2C + C_Z + C_P$$

$$[C_1]=\begin{bmatrix} C_P \\ C_P \\ C_P \\ \vdots \\ C_P \\ C_P + C \end{bmatrix} \quad , [\underline{U}]=\begin{bmatrix} \underline{U}_1 \\ \underline{U}_2 \\ \underline{U}_3 \\ \vdots \\ \underline{U}_{n-2} \\ \underline{U}_{n-1} \end{bmatrix}$$

Matrix $[C]$ has dimensions (n-1)×(n-1), vector $[C_1]$ has dimensions (n-1)×1, vector $[\underline{U}]$ has dimensions (n-1)×1.

Voltage drop at i-th disc insulator can be calculated by using equation (8):

$$U_{Di} = U_i - U_{i-1} \tag{8}$$

where: i=1, …, n, $U(0)=0$ and $U(n)=U$.

Values of parasite capacitances C_Z, C_P and C can be calculated in that way that difference between measured and calculated results is minimum, equation (9):

$$\min\left\{\text{sum}\left[\text{abs}\left(U_M - U_C\right)\right]\right\} \tag{9}$$

where: U_M is vector of measured voltages at disc insulators, Table III, and U_C is vector of calculated voltages at disc insulators.

Calculation of parasite capacitances is performed in two ways:

- Case 1 - Calculations are performed at the insulator string composed of six disc insulators. Following optimal values of parasite capacitances are calculated: C_Z=4.5 pF, C_P=1.6 pF, C=40 pF. These values are applied for all other insulator strings. Estimated results of voltage distributions along the cap-and-pin insulators are presented in Table IV.
- Case 2 - Calculations are performed separately for all five insulators strings. Disc insulator parasite self-capacitance is assumed to be C=40 pF in all calculations, as calculated in case 1. Following optimum parasite capacitances values are estimated:
  - 6 disc insulators in string: C_Z=4.5 pF, C_P=1.6 pF.
  - 5 disc insulators in string: C_Z=4.4 pF, C_P=1.5 pF.
  - 4 disc insulators in string: C_Z=5.8 pF, C_P=2.5 pF.
  - 3 disc insulators in string: C_Z=3.8 pF, C_P=2.8 pF.
  - 2 disc insulators in string: C_Z=5.5 pF, C_P=1.5 pF.

  In the case of insulator string composed of two discs, there are a lot of possible combinations of parasite capacitances values C_Z and C_P which allow estimation of the minimum difference between measured and calculated results. Results estimated by using foregoing mentioned parasite capacitances' values are presented in Table V.

Similar values of parasite capacitances as in case 1 and case 2 are applied in [12].

TABLE IV. CALCULATED VOLTAGE DISTRIBUTION ALONG THE CAP-AND-PIN INSULATORS BY USING ANALYTICAL MODEL – CASE 1

Disc number	**Voltage distribution at cap-and-pin insulator [pu]**				
	Number of disc insulators in the insulator string				
	II discs	III discs	IV discs	V discs	VI discs
I*	48.32	30.99	22.43	17.49	14.41
II	51.68	31.72	21.85	16.15	12.61
III		37.28	24.61	17.28	12.73
IV			31.11	21.05	14.79
V				28.03	19.11
VI					26.34

I* - disc near the earthed electrode

TABLE V. CALCULATED VOLTAGE DISTRIBUTION ALONG THE CAP-AND-PIN INSULATORS BY USING ANALYTICAL MODEL – CASE 2

Disc number	**Voltage distribution at cap-and-pin insulator [pu]**				
	Number of disc insulators in the insulator string				
	II discs	III discs	IV discs	V discs	VI discs
I*	47.51	33.13	22.74	17.36	14.41
II	52.49	31.57	21.21	16.17	12.61
III		35.28	24.09	17.36	12.73
IV			31.96	21.12	14.79
V				27.99	19.11
VI					26.34

I* - disc near the earthed electrode

Relative errors between the measured results from Table III and calculated results from Table IV and Table V are presented in Table VI and Table VII respectively. Calculations of the relative error for i-th disc insulator (RE_i) is performed by using equation (10):

$$RE_i = \frac{U_{Ci} - U_{Mi}}{U_{Mi}} \cdot 100\% \tag{10}$$

where: U_{Ci} is calculated voltage value at i-th disc insulator and U_{Mi} is measured voltage value at i-th disc insulator.

Calculated errors in Tables VI and VII are in the acceptable range [1]. It is important to take into account that measurement results from Table III have some errors, as discussed in section II. In the case 2, Table VII, better agreement between the measured and calculated results is achieved in comparison with the case 1, Table V, because in case 2 optimum values of

parasite capacitances' C_Z and C_P are estimated for every insulator string.

TABLE VI. RELATIVE ERRORS BETWEEN MEASURED AND CALCULATED VOLTAGE DISTRIBUTION ALONG THE CAP-AND-PIN INSULATORS FOR CASE 1

Disc number	**Relative error between calculated and measured results [%]**				
	Number of disc insulators in the insulator string				
	II discs	III discs	IV discs	V discs	VI discs
I*	3.27	-5.81	-1.04	0.82	-0.12
II	-0.69	7.29	3.89	3.71	0.14
III		5.99	5.44	5.04	-1.03
IV			-2.40	-0.53	-2.42
V				0.85	10.54
VI					-0.06

I* - disc near the earthed electrode

TABLE VII. RELATIVE ERRORS BETWEEN MEASURED AND CALCULATED VOLTAGE DISTRIBUTION ALONG THE CAP-AND-PIN INSULATORS FOR CASE 2

Disc number	**Relative error between calculated and measured results [%]**				
	Number of disc insulators in the insulator string				
	II discs	III discs	IV discs	V discs	VI discs
I*	1.54	0.69	0.32	0.08	-0.12
II	0.86	6.78	0.85	3.84	0.14
III		0.31	3.21	5.52	-1.03
IV			0.27	-0.20	-2.42
V				0.71	10.54
VI					-0.06

I* - disc near the earthed electrode

IV. NUMERICAL CALCULATION OF THE VOLTAGE DISTRIBUTION ALONG THE CAP-AND-PIN INSULATORS

Numerical calculations of the voltage distribution along the insulators can be done by using specialized software [1],[3],[7],[13]. In this paper software Comsol Multiphysics is used [10]. Electrostatic mathematical model and 2D axisymmetric geometry are applied [3],[13],[15],[16]. Laplace equation (11) is used to describe electrostatic field:

$$\varepsilon_0 \cdot \varepsilon_r \cdot \mathrm{div}(\mathrm{grad}V) = 0 \qquad (11)$$

where: ε_r is relative permittivity of the material, ε_0 is permittivity od vacuum $\varepsilon_0 \approx 8.855 \times 10^{-12}$ F/m, V – electric potential [V].

Graphical representation of the voltage distribution around the insulator string composed of two disc insulators is presented in Fig 6.

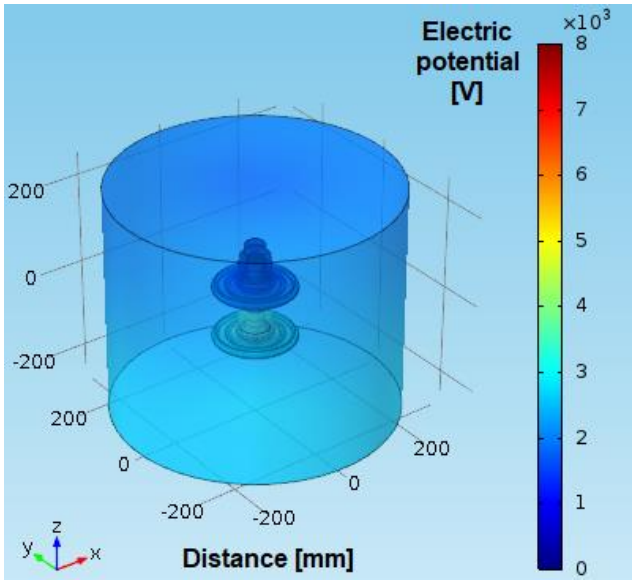

a)

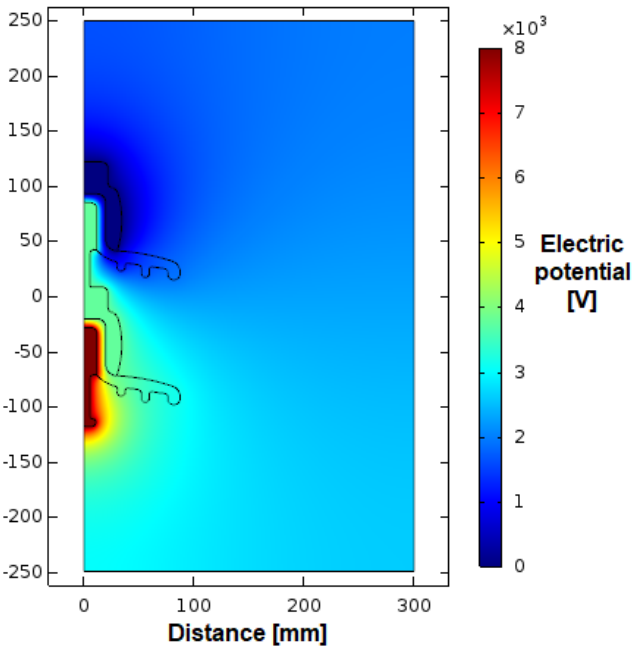

b)

Figure 6. Voltage distribution around the insulator string composed of two disc insulators: a) 3D view, b) 2D view

Graphical representation of the voltage and electric field intensity along the axis of the insulator string composed of two disc insulators is presented in Fig 7. Electrostatic field intensity in conducting materials (aluminum) is equal zero, Fig. 7 b), and consequently electric potential is such materials is constant, Fig. 7 a). Electric field exist in dielectrics (air and glass), Fig. 7 b), and consequently all voltage drop appears in dielectrics, Fig. 7 a). The same situation is in the case of insulators strings consisting of more than two disc insulators.

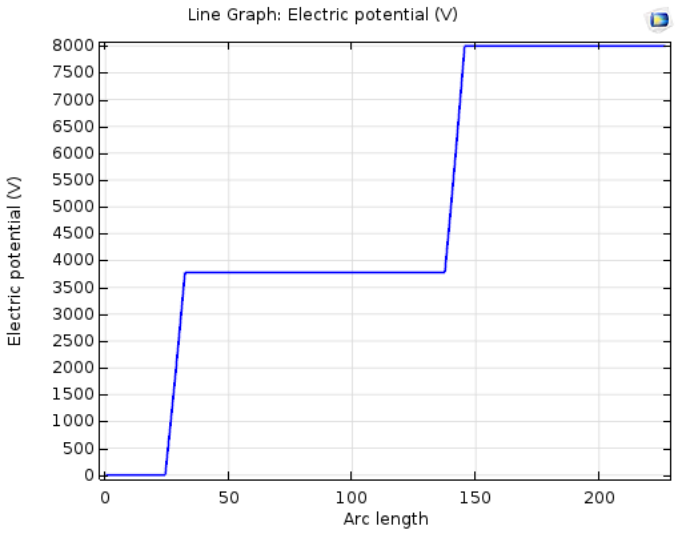

a)

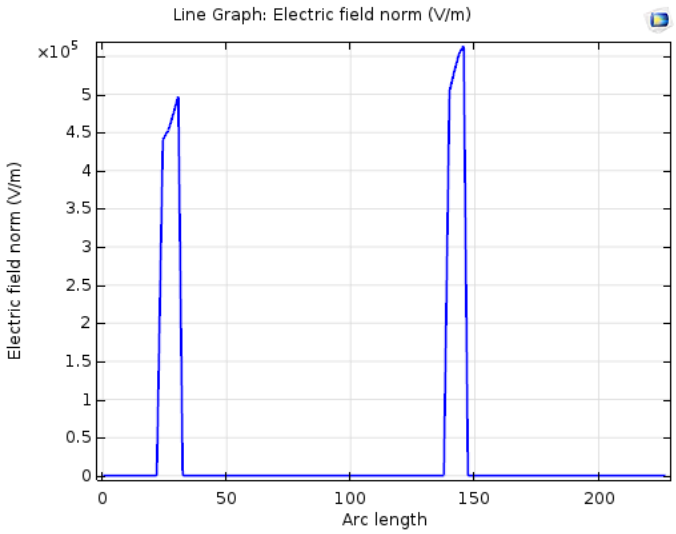

b)

Figure 7. Graphical representation of the a) voltage, b) electric field intensity along the axis of the insulator string composed of two disc insulators

Graphical representation of the voltage distribution around the insulator string composed of six disc insulators is presented in Fig 8.

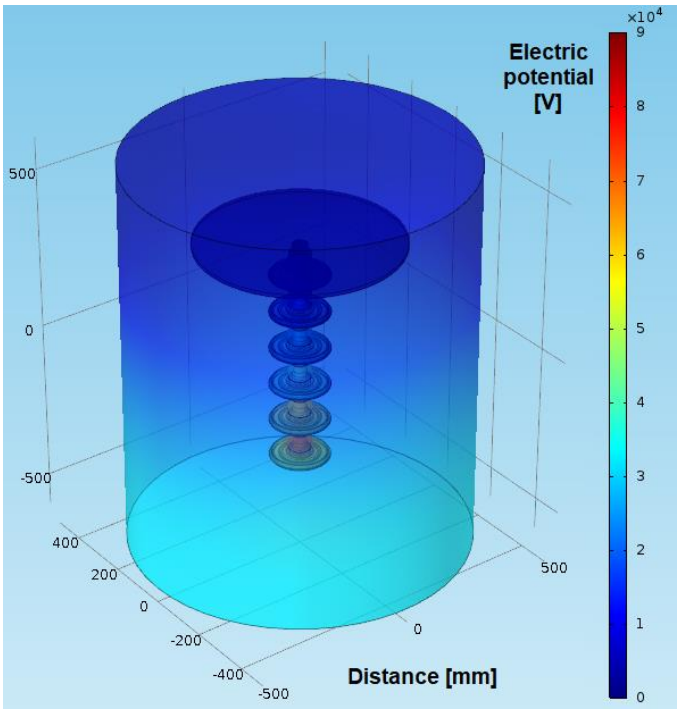

a)

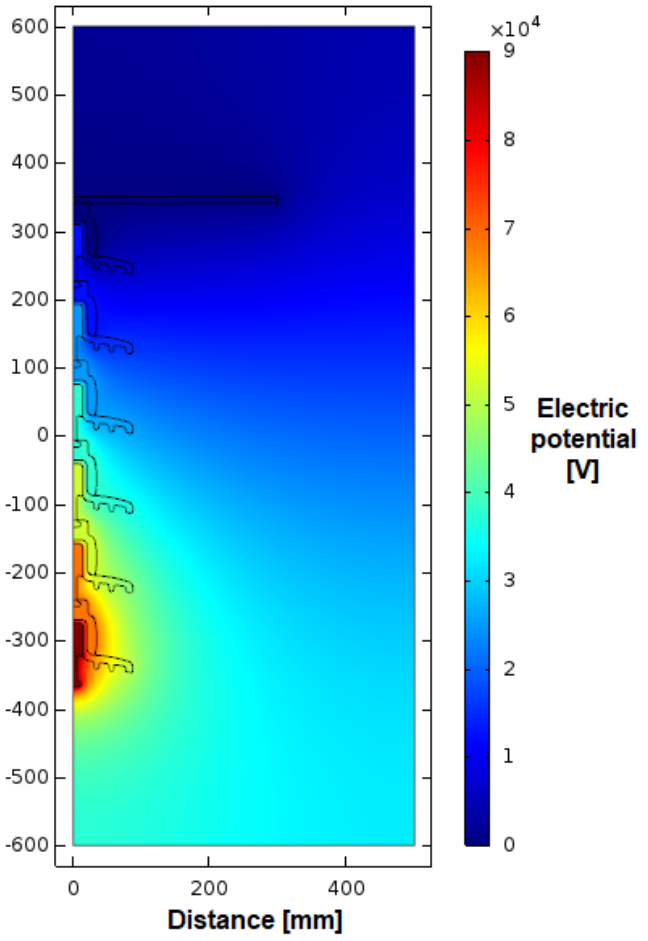

b)

Figure 8. Voltage distribution around the insulator string composed of six disc insulators: a) 3D view, b) 2D view

Graphical representation of the voltage and electric field intensity along the axis of the insulator string composed of six disc insulators is presented in Fig 9.

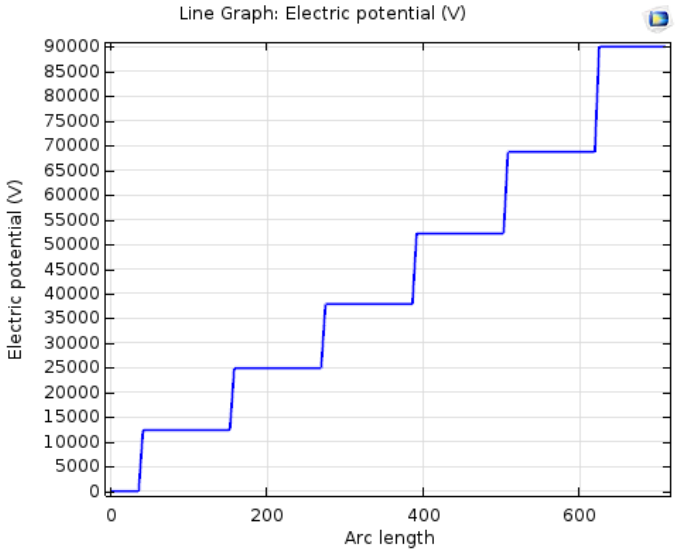

a)

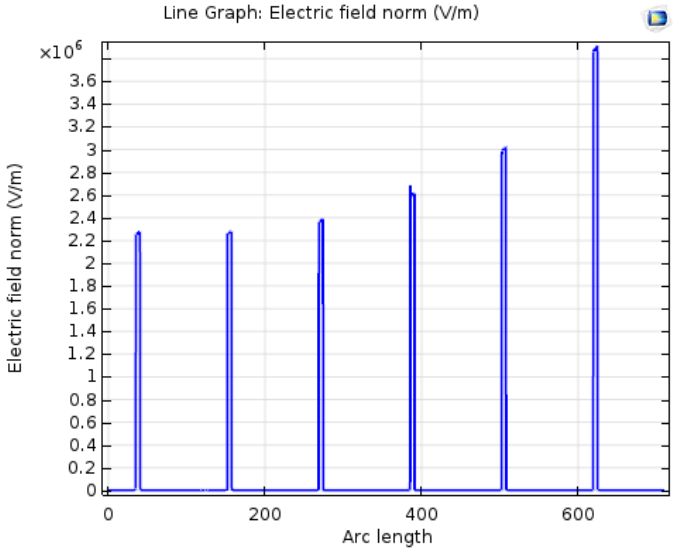

b)

Figure 9. Graphical representation of the a) voltage, b) electric field intensity along the axis of the insulator string composed of six disc insulators

Measuring configuration from Fig. 4 a) is not suitable for numerical analysis because of the huge supporting structure for the insulators strings, as well as because of the connecting conductors placed perpendicularly to the insulator string. These elements impact electric field distribution around the insulator string and consequently voltage distribution along the insulator string. Exact 3D modeling of measuring configuration from Fig. 4 a) is very complicate, and numerical calculations in such 3D model require powerful computer system. If analyzed geometry has axial symmetry the same calculation accuracy can be obtained by using 2D axisymmetric models as by using 3D models [15],[16]. 2D axisymmetric models allow users to simplify calculation procedure and avoid complicate 3D geometries. However, measuring setup geometry presented in Fig. 4 a) is partially axisymmetric and application of 2D axisymmetric model introduce limitations connected with representation of exact measuring setup geometry, especially geometry of the insulator string supporting system.

Results of numerical calculations related to the voltage distribution along the insulators strings are presented in Table VIII. Relative errors between the measured results from Table III and calculated results from Table VIII are presented in Table IX. Calculations of the relative error for *i*-th disc insulator is performed by using equation (10). In this case relative errors between measured and calculated results of voltage distribution along the insulators strings are higher than in the analytical calculations, section III, especially in the case of longer insulators strings, Table VI and Table VII. This is probably caused by application of the 2d axisymmetric geometry instead of 3D model in numerical calculations as well as by the errors in measurement results. Despite that, errors of the calculated results are still acceptable. As presented in [1], despite exact 3D model of the measuring setup configuration is implemented in software errors between the measured and calculated results rich 6%.

In order to estimate valuable results, in the case when number of disc insulators is four, five and six, metal plate at the grounded side of the insulator string must be added, as in Fig. 8. This metal plate represents insulator string supporting structure and grounding conductor.

TABLE VIII. CALCULATED VOLTAGE DISTRIBUTION ALONG THE CAP-AND-PIN INSULATORS BY USING SPECIALIZED SOFTWARE

Disc number	**Voltage distribution at cap-and-pin insulator [pu]**				
	Number of disc insulators in the insulator string				
	II discs	III discs	IV discs	V discs	VI discs
I*	48.20	32.10	22.10	17.00	13.8
II	51.80	31.80	22.55	17.20	13.85
III		36.10	24.75	18.40	14.45
IV			30.60	20.90	15.9
V				26.50	18.3
VI					23.7

I* - disc near the earthed electrode

TABLE IX. RELATIVE ERRORS BETWEEN MEASURED AND CALCULATED VOLTAGE DISTRIBUTION ALONG THE CAP-AND-PIN INSULATORS

Disc number	**Relative error between calculated and measured results [%]**				
	Number of disc insulators in the insulator string				
	II discs	III discs	IV discs	V discs	VI discs
I*	3.02	-2.44	-2.50	-2.00	-4.35
II	-0.46	7.56	7.22	10.45	9.99
III		2.64	6.04	11.84	12.34
IV			-4.00	-1.24	4.91
V				-4.65	5.85
VI					-10.08

I* - disc near the earthed electrode

V. COMPARISON OF ESTIMATED RESULTS

Differences between the measured and calculated results can be graphically compared as presented in Fig. 10. Marks in Fig. 10 have following meanings:

- MR – measurement result,
- AC-case 1 – analytical calculation-case 1,
- AC-case 2 – analytical calculation-case 2,
- NC – numerical calculation.

With I* in Fig. 10 is marked disk insulator near the earthed electrode.

It can be concluded that satisfying agreement between the measured and calculated results are achieved, so the presented analytical and numerical models are correct, but also easy to use. In order to improve accuracy of estimated results in analytical calculations it is possible to consider variation of the parasite capacitances' values C_Z and C_P along the disc insulators. Accuracy of the results estimated in numerical calculations can be improved by drawing and analyzing exact 3D geometry as that of the measuring test system.

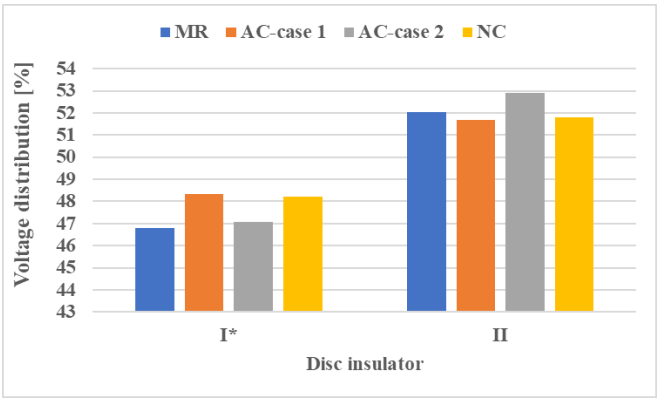

a)

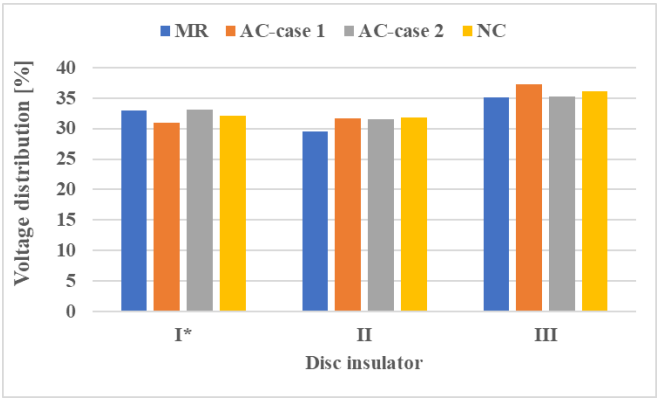

b)

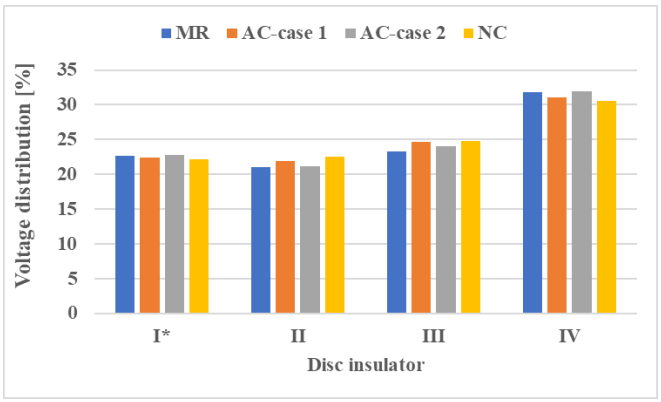

c)

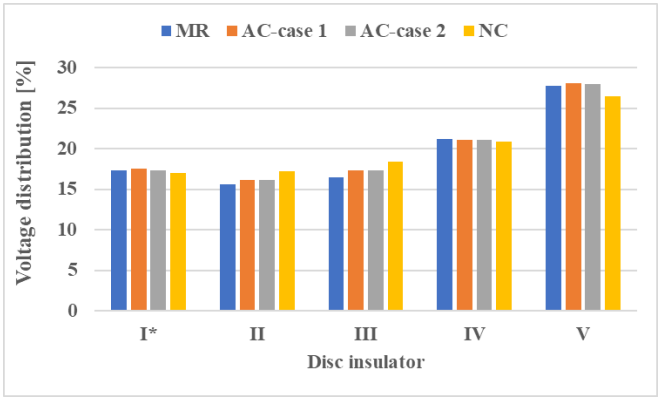

d)

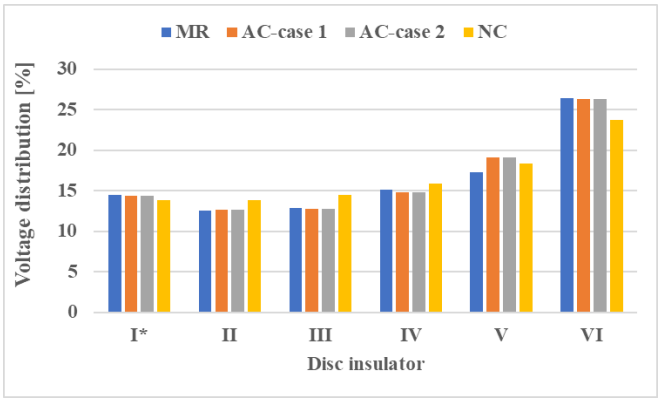

e)

Figure 10. Voltage distribution along the insulator string composed of: a) two, b) three, c) four, d) five, e) six) U40BL glass disc insulators

VI. CONCLUSION

In this paper the experimental, analytical and numerical analysis of the non-linear voltage distribution along the five different cap-and-pin insulators composed of U40BL glass disc insulators are presented. Performed analyses can hardly be found in the literature, summarized in one paper. Experimental measurement is performed by using simple and low-cost measuring equipment and it is suitable for application in all high voltage laboratories. Additionally, measuring procedure is well explained and it can be easily reused by other authors. Analytical mathematical model is discussed in detail, and

procedure for estimation values of parasite capacitance based on the measurement results is given. Numerical analysis is performed in specialized software Comsol Multyphisics and by using electrostatic 2D axisymmetric model of the system. This model is much easier to implemented compared to 3D model, while it allows estimation of results which are in good agreement with those of experimental measurement. Correctness of the presented analytical and numerical calculation procedures is verified through comparison with experimentally obtained results.

REFERENCES

[1] V. T. Kontargyri, L. N. Plati, I. F. Gonos, I. A. Stathopulos, "Measurement and simulation of the voltage distribution and the electric field on a glass insulator string," Measurement, vol. 41, pp. 471–480, 2008.

[2] D. Train, R. Dube, "Measurements of Voltage Distribution on Suspension Insulators for HVDC Transmission Lines", IEEE Transactions on Power Apparatus and Systems, vol. PAS-102, no. 8, pp. 2461-2475, August 1983.

[3] M. Banjanin, B. Novaković, "Numerical analyses of the selected high voltage electrostatic problems and configurations," 2020 19th International Symposium INFOTEH-JAHORINA, March 2020, East Sarajevo, Bosnia and Herzegovina.

[4] K. Yamada, A. Hayashi, C. Saka, K. Sakanishi, R. Matsuoka, "Improvement of Contamination Flashover Voltage Performance of Cylindrical Porcelain Insulators", Conference Record of the 2008 IEEE International Symposium on Electrical Insulation, Vancouver, BC, Canada, June 2008.

[5] K. Siderakis, D. Agoris, J. Stefanakis, E. Thalassinakis, "Influence of the profile on the performance of porcelain insulators installed in coastal high voltage networks in the case of condensation wetting", IEE Proceedings - Science, Measurement and Technology, vol. 153, no. 4, pp. 158-163, July 2006.

[6] Z. Zhang. S. Yang, X. Jiang, X. Qiao, Y. Xiang, D. Zhang, "DC Flashover Dynamic Model of Post Insulator under Non-Uniform Pollution between Windward and Leeward Sides", Energies, vol. 12, 2345, 2019.

[7] E. Akbari, M. Mirzaie, A. Rahimnejad, M. B. Asadpoor, "Finite Element Analysis of Disc Insulator Type and Corona Ring Effect on Electric Field Distribution over 230-kV Insulator Strings", International Journal of Engineering and Technology, vol. 1, no. 4, pp. 407-419, 2012.

[8] M. Izadi, M. S. B. Abd Rahman, M. Z. A. Ab Kadir, "On the voltage and electric field distribution along polymer insulator", 2014 IEEE 8th International Power Engineering and Optimization Conference, Langkawi, Malaysia, March 2014.

[9] K. Katada, Y. Takada, M. Takano, T. Nakanishi, Y. Hayashi, R. Matsuoka, "Corona discharge characteristics of water droplets on hydrophobic polymer insulator surface", Proceedings of the 6th International Conference on Properties and Applications of Dielectric Materials, Xi'an, China, June 2000.

[10] COMSOL Multiphysics®, www.comsol.com. COMSOL AB, Stockholm, Sweden.

[11] S. M. Al Dhalaan, M. A. Elhirbawy, "Simulation of Voltage Distribution Calculation Methods Over a String of Suspension Insulators", 2003 IEEE PES Transmission and Distribution Conference and Exposition, Dallas, USA, September 2003.

[12] K. L. Chrzan, W. Rebizant, "PSPICE Application for Modelling of Cap and Pin Insulator Strings", International Conference Modern Electric Power Systems, September 2002.

[13] M. Banjanin, M. Savić, "Tehnika visokog napona 2 – auditorne, numeričke i laboratorijske vježbe", Univerzitet u Istočnom Sarajevu, Elektrotehnički fakultet, str. 224, 2019 (in Serbian).

[14] M. Beyer, W. Boeck, K. Moeller, W. Zaengl, "High Voltage Engineering", Springer Verlag, Berlin 1986.

[15] C. Volat, M. Farzaneh, "A Simple Axisymmetric Model for Calculation of Potential Distribution along Ice-Covered Post Station Insulators during a Melting Period", 2008 Annual Report Conference on Electrical Insulation and Dielectric Phenomena, Quebec, Canada, October 2008.

[16] C. Volat, H. Ezzaidi, I. Fofana, "Comparison Between 2D and 3D Modeling of an EHV Post Station Insulator Equipped with a Grading Ring", 2013 Electrical Insulation Conference, Ottawa, Ontario, Canada, June 2013.

Mladen Banjanin received his BSc degree in 2011 from the Faculty of Electrical Engineering in East Sarajevo, Bosnia and Herzegovina, and MSc and PhD degrees in 2012 and 2017 years, respectively, from the School of Electrical Engineering in Belgrade, Serbia. He is an assistant professor, head of the Department of Electric Power Systems and vice dean at the Faculty of Electrical Engineering in East Sarajevo. His main area of interest covers high voltage engineering and lighting protection.